Preprints.org

Review

Not peer-reviewed version

Improvement of Algan Homoepitaxial Tunnel Junction Deep-UV Light-Emitting Diodes by Controlling the Growth of N-Type Algan and Polycrystalline Mgzno/Al Electrodes

Kengo Nagata * , Taichi Matsubara , Yoshiki Saito , Keita Kataoka , Tetsuo Narita , Kayo Horibuchi , Maki Kushimoto , Shigekazu Tomai , Satoshi Katsumata , Yoshio Honda , Tetsuya Takeuchi , Hiroshi Amano

Posted Date: 15 February 2023

doi: 10.20944/preprints202302.0249.v1

Keywords: AlGaN; tunnel junction; light-emitting diode; deep-ultraviolet; MgZnO

Preprints.org is a free multidiscipline platform providing preprint service that is dedicated to making early versions of research outputs permanently available and citable. Preprints posted at Preprints.org appear in Web of Science, Crossref, Google Scholar, Scilit, Europe PMC.

Copyright: This is an open access article distributed under the Creative Commons Attribution License which permits unrestricted use, distribution, and reproduction in any medium, provided the original work is properly cited.

Preprints (www.preprints.org) | NOT PEER-REVIEWED | Posted: 15 February 2023 doi:10.20944/preprints202302.0249.v1

Disclaimer/Publisher's Note: The statements, opinions, and data contained in all publications are solely those of the individual author(s) and contributor(s) and not of MDPI and/or the editor(s). MDPI and/or the editor(s) disclaim responsibility for any injury to people or property resulting from any ideas, methods, instructions, or products referred to in the content.

Review

Improvement of AlGaN Homoepitaxial Tunnel Junction Deep-UV Light-Emitting Diodes by Controlling the Growth of n-Type AlGaN and Polycrystalline MgZnO/Al Electrodes

Kengo Nagata [1,*], Taichi Matsubara [2], Yoshiki Saito [1], Keita Kataoka [3], Tetsuo Narita [3], Kayo Horibuchi [3], Maki Kushimoto [2], Shigekazu Tomai [4], Satoshi Katsumata [4], Yoshio Honda [5], Tetsuya Takeuchi [6] and Hiroshi Amano [5]

[1] Toyoda Gosei Co., Ltd., 710 Shimomiyakeoriguchi, Heiwa-cho, Inazawa, Aichi 290-1312, Japan; kengo.nagata@toyoda-gosei.co.jp, yoshiki.saito@toyoda-gosei.co.jp
[2] Graduate School of Engineering, Nagoya University, Furo-cho, Chikusa-ku, Nagoya, Aichi 464-8603, Japan; matsubara.taichi@i.mbox.nagoya-u.ne.jp, kushimoto@nuee.nagoya-u.ac.jp
[3] Toyota Central R&D Labs. Inc., Nagakute, Aichi 480-1192, Japan; e1354@mosk.tytlabs.co.jp, tetsuo-narita@mosk.tytlabs.co.jp, e4721@mosk.tytlabs.co.jp
[4] Advanced Technology Research Laboratories, Idemitsu Kosan Co., Ltd., 1280 Kamiizumi, Sodegaura, Chiba 299-0205, Japan; shigekazu.tomai.6560@idemitsu.com, satoshi.katsumata.6820@idemitsu.com
[5] Center for Integrated Research of Future Electronics, Institute of Materials and Systems for Sustainability, Nagoya University, Furo-cho, Chikusa-ku, Nagoya, Aichi 464-8601, Japan; honda@nagoya-u.jp, amano@nuee.nagoya-u.ac.jp
[6] Faculty of Science and Technology, Meijo University, 1-501 Shiogamaguchi, Tenpaku-ku, Aichi 468-8502, Japan; take@meijo-u.ac.jp
* Correspondence: kengo.nagata@toyoda-gosei.co.jp

Abstract: Deep-ultraviolet (UV) light-emitting diodes (LEDs) based on AlGaN crystals have low light-emission efficiency; therefore, there is a need to improve this light-emission efficiency for a wide range of applications such as water and air sterilizations. UV-light-transparent device structures are considered one of the many solutions toward increasing light output power. To this end, the present study focused on developing a transparent AlGaN-based tunnel junction (TJ) as the anode of a deep-UV LED. Deep-UV LEDs composed of n^+/p^+-type AlGaN TJs were fabricated under the growth condition that reduced the carrier compensation in the n^+-type AlGaN layers. The operating voltage was 10.8 V under the direct current (DC) operation of 63 A/cm^2. In addition, magnesium zinc oxide (MgZnO)/Al reflective electrodes were fabricated to enhance the output power of the AlGaN homoepitaxial TJ LED. The output power was 57.3 mW under a DC operation of 63 A/cm^2, and it was 1.7 times higher than that realized using the conventional Ti/Al electrodes. The combination of the AlGaN-based TJ and MgZnO/Al reflective contact allows further improvement of the light output power. This study confirms that the AlGaN TJ is a promising UV-transmittance structure that can obtain a high light-extraction efficiency.

Keywords: AlGaN; tunnel junction; light-emitting diode; deep-ultraviolet; MgZnO

1. Introduction

Aluminum gallium nitride (AlGaN)-based light-emitting diodes (LEDs) emit deep-ultraviolet (UV) light and are utilized in several applications at different wavelengths such as in curing, sensing, and water and air sterilizations. These LEDs are considered replacements for the mercury lamps used in water and air sterilizations [1–3]. Deep-UV light with an emission wavelength below 290 nm can rapidly inactivate the deoxyribonucleic acid of virus and bacteria [4,5]; however, the light-emission efficiency (LEE) of deep-UV LEDs is considerably lower than that of low-pressure mercury lamps.

© 2023 by the author(s). Distributed under a Creative Commons CC BY license.

 doi:10.20944/preprints202302.0249.v1

The wall-plug efficiency of mass-produced deep-UV LEDs is a maximum of 10% because of the UV light absorption of the p-type gallium nitride (GaN) contact layer [6–8]. A p-type GaN contact layer is used in mass-produced deep-UV LEDs because a higher Al composition p-type AlGaN can lead to a higher ionization energy of magnesium (Mg) acceptors and a lower hole concentration [9–14]. AlGaN homoepixial tunnel junction (TJ) LEDs without a GaN or gallium indium nitride (GaInN) layer have been reported by several research groups for enhancing the light-extraction efficiency (LEE) of deep-UV LEDs; the LEE is high, and the device operates at a voltage of 13–50 V [15,16]. Further, it is necessary to increase the high Si-doping concentration at the TJ layer to increase tunnel probability. The resistivity of the high-Al-composition n-type AlGaN layer with a high Si-doping concentration (>6 × 10^{19} cm^{-3}) is extremely high because of the self-compensation caused by the cation–vacancy–silicon (V_{III}–nSi) complexes [17–22]. Further, carbon atoms possibly cause carrier compensation by substituting nitrogen sites (C_N), which can reduce conductivity in n-type GaN [23]. The growth condition of the high-Si-doped n^+-type AlGaN needs to be controlled for suppressing the carrier compensation defects and reducing the operating voltage of AlGaN TJ LEDs.

In addition, UV light absorption occurs at electrodes, and we focus on high-Al composition AlGaN TJ LEDs and magnesium zinc oxide (MgZnO)/Al reflective electrode [24,25]. MgZnO is suitable for suppressing light absorption, and this can help widen the band gap from 3.34 to 7.8 eV by controlling the Mg composition in MgZnO. A previous study reported that sputtered MgZnO exhibited two crystalline structures after recrystallization by annealing; both structures exhibited high transmittance in the UV range and n-type conductivity [26].

In this study, we review key challenges of AlGaN TJ deep-UV LEDs. The growth conditions of the n^+-type AlGaN of TJ are controlled such that carbon incorporation can be suppressed at high Si doping to reduce the operating voltage of the AlGaN TJ LED. Further, we demonstrate that MgZnO/Al reflective electrodes can fully exploit the transparent structure of TJs, which results in enhancing the LEE of deep-UV LEDs.

2. Materials and Methods

Deep-UV LEDs were grown using a metalorganic vapor phase epitaxy on c-plane sapphire substrates with a miscut angle of 0.35° toward the sapphire [11$\bar{2}$0] direction. Trimethylaluminium, trimethylgallium, triethylgallium, Bis(cyclopentadienyl)magnesium, monosilane gas, and ammonia gases were used as Al, Ga, Mg, Si, and N sources under hydrogen gas, respectively. The sapphire substrates were thermally cleaned in the H_2 ambient, and then, a 3-μm-thick AlN was grown using a two-step growth technique [27]. Threading dislocation densities of screw and edge dislocations including mixed components in the AlN underlayer were estimated using an X-ray rocking curve at 9 × 10^7 cm^{-2} and 1 × 10^9 cm^{-2}, respectively [28]. The 1.3-μm-thick n-type $Al_{0.62}Ga_{0.38}N$ doped with a Si concentration of 3 × 10^{19} cm^{-3} was grown on an AlN template [21,22]. Multiple-quantum wells, an $Al_{0.85}Ga_{0.15}N$ electron blocking layer (EBL), a p-type AlGaN, and a p^+-type AlGaN were grown on the n-type AlGaN underlayer. The p^+-type AlGaN was doped with Mg at a concentration of 1.7 × 10^{20} cm^{-3}. Subsequently, n^+-type and n-type AlGaN were grown under the same conditions as those of the n-type AlGaN underlayer, as indicated in Figure 1b. The mesa was formed by dry etching using HCl gas. Thereafter, we formed 20/150/50/100/240-nm-thick V/Al/Ti/Pt/Au electrodes as both n-type AlGaN electrodes, and they were simultaneously annealed under a nitrogen (N_2) ambient at 720 °C for 30 s. Further, the annealing process contributes Mg activation under lateral hydrogen diffusion from the exposed mesa-parts of the p-type layers [29–33]. For comparison, we prepared a conventional pn-diode-based LED with a thin p-type GaN contact layer grown on a p-type AlGaN shown in Figure 1a. We adopted indium zinc oxide (IZO) for the anode. The emitted UV light was fully absorbed at the IZO electrode; the sizes of the LED and the anode, and the thickness of the sapphire substrate were 1 mm^2, 0.56 mm^2, and 200 μm, respectively. The light output power was measured using an integrating sphere. For the former, we prepared an AlGaN homoepitaxial TJ LED (TJ#1 to TJ#5) with various Si concentrations and C incorporations in the n^+-type AlGaN layer, as summarized in Table 1. The carbon concentration was approximately 3.0 × 10^{18} cm^{-3} (TJ#1 and TJ#2), and it was reduced to 6.5 × 10^{17} cm^{-3} (TJ#3 to TJ#5) by changing the growth pressure from 50 mbar to

100 mbar. In case of the latter, we prepared MgZnO/Al electrodes for the TJ LED with TJ#5. We deposited a 50-nm-thick MgZnO electrode by RF magnetron sputtering at a substrate temperature of 200 °C, and a typical lift-off process was employed. The sputtering target for MgZnO was prepared as a 2-inch MgZnO sintered material of purity 4N, which is the MgO:ZnO mixing atomic ratio of 1:2. The RF power, sputtering gas, and gas pressure were 100 W, Ar, and approximately 3.4–3.5 × 10^{-1} Pa, respectively. After forming the MgZnO electrode, the conductivity was improved by annealing at 850 °C for 5 min under N_2 ambient. In the cathode, Ti/Al electrodes were deposited by the electron beam (EB) method and alloyed at 450 °C under N_2 ambient. Al/Ti/Pt/Au electrodes with 300/50/100/240 nm were formed on the MgZnO electrode via the EB method to obtain a high-reflective electrode. The reflectance of the electrodes for TJ LEDs was measured using a UV-visible spectrophotometer (UV-VIS). For comparison, Ti/Al electrodes for the TJ LED anode were prepared via the same process as the cathode.

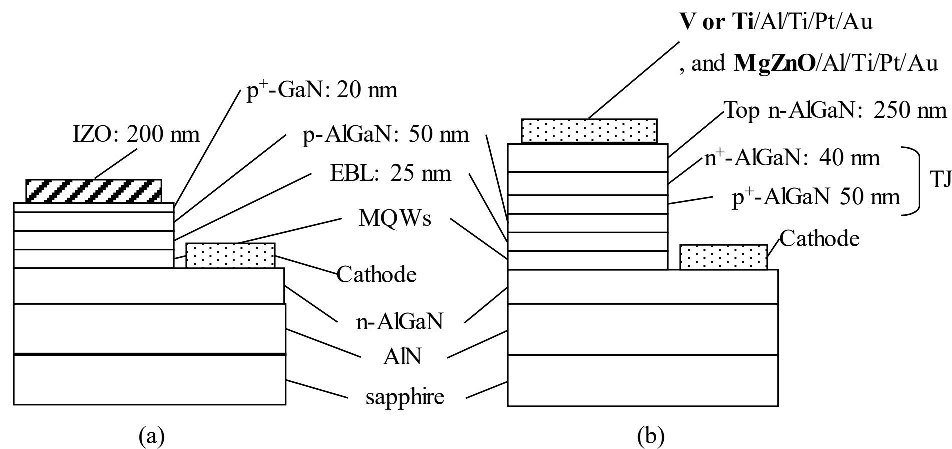

Figure 1. Deep-UV LED structures for (a) PN junction and (b) TJ devices.

Table 1. Summary of the evaluated parameters for all LEDs. PN and TJ indicate the PN junction and TJ LEDs, respectively. [Si] and [C] are directly measured for the samples TJ#1, TJ#3, and TJ#4, whereas [Si] and [C] in samples TJ#2 and TJ#5 (labeled by*) are estimated from the dates for TJ#1, TJ#3, and TJ#4. Copyright 2021 The Japan Society of Applied Physics [34].

Sample		p-AlGaN	p^+-AlGaN	n^+-AlGaN	
		Al composition		[Si] (cm^{-3})	[C] (cm^{-3})
PN	#1	50%	50%		
	#2	50%	50%		
TJ	#1	50%	50%	6.3×10^{19}	1.8×10^{18}
	#2	50%	50%	1.3×10^{20}*	1.8×10^{18}*
	#3	50%	50%	6.3×10^{19}	3.1×10^{17}
	#4	50%	50%	1.3×10^{20}	3.1×10^{17}
	#5	60%	60%	1.3×10^{20}*	3.1×10^{17}*

3. Results and Discussions

3.1. AlGaN Homoepitaxial Tunnel-Junction Deep-UV LEDs with n-Type AlGaN based on Suppressed Complex Defect Formation

Forward voltage–current density characteristics for samples PN#1, TJ#1, TJ#2, TJ#3, and TJ#4 are presented in Figure 2 and measured by direct current (DC) operation at 300 K. The forward voltage (6.6 V) of the conventional PN LED (PN#1) was provided at 63 A/cm^2. The characteristics were roughly the same as those reported previously [35–37]. The forward voltage of the TJ LEDs (TJ#1 and TJ#2) was extremely high and operated at approximately 16 V at 4 A/cm^2. These TJ LEDs could not perform sufficient current injection; however, a slightly decreasing forward voltage trend was

Preprints (www.preprints.org) | NOT PEER-REVIEWED | Posted: 15 February 2023 doi:10.20944/preprints202302.0249.v1

observed for TJ#2 relative to TJ#1. Forward voltages of TJ#3 and TJ#4 were 12.1 V and 10.3 V at 63 A/cm^2, respectively, and this was significantly reduced by more than 6 V than those of TJ#1 and TJ#2. The high-doping Si concentration of the n$^+$-type AlGaN was effective in reducing the forward voltage of the AlGaN TJ LEDs. Further, suppressing the C incorporation was more effective than the high Si-doping concentration of the n$^+$-type AlGaN in reducing the forward voltage. The operating voltage of AlGaN TJ LEDs could be reduced because the carrier concentration of n$^+$-type $Al_{0.6}Ga_{0.4}N$ was increased by suppressing the C incorporation. The electrical characteristics of the n-type AlGaN at 300 K under the van der–Pauw Hall effect were measured. The carrier concentration and resistivity of the n$^+$-type $Al_{0.6}Ga_{0.4}N$ with a Si concentration of 1.2 × 10^{20} cm^{-3} based on TJ#2 was extremely low (< 1.0 × 10^{16} cm^{-3}) and semi-insulating because of the compensation by C_N, as shown in Figure 3a and ref. [34]. Those at a Si concentration of 1.2 × 10^{20} cm^{-3} based on TJ#4 were 3.5 × 10^{16} cm^{-3} and 23 Ωcm, respectively, because of the suppression of C incorporation in the n$^+$-type AlGaN. This improvement contributes to the reduction in the forward voltage for TJ#4 compared to TJ#2.

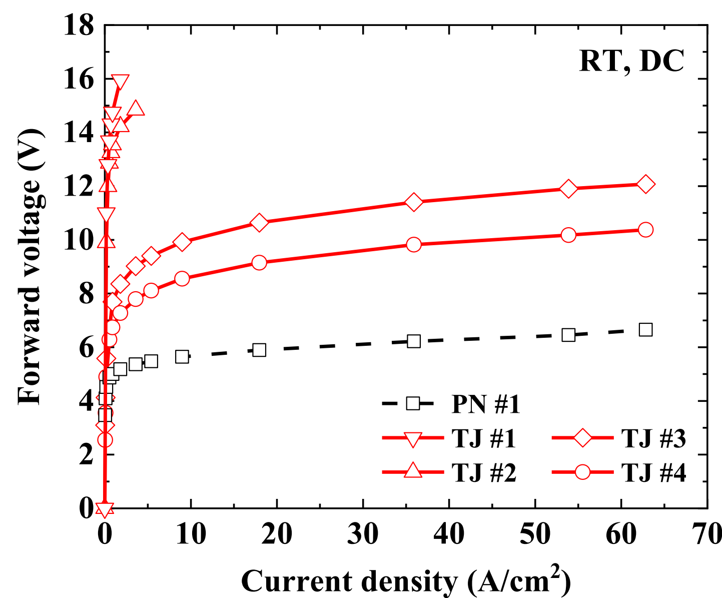

Figure 2. Forward voltage–current density characteristics measured by DC operation at room temperature for samples PN#1, TJ#1, TJ#2, TJ#3, and TJ#4. Copyright 2021 The Japan Society of Applied Physics. [34].

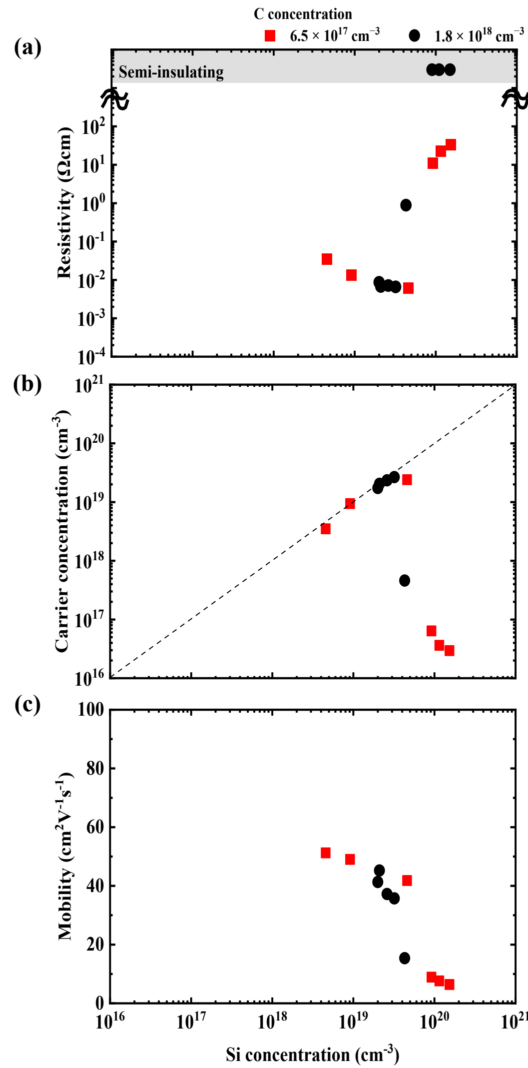

Figure 3. Si concentration dependence of (**a**) resistivity, (**b**) carrier concentration, and (**c**) mobility of n-type $Al_{0.62}Ga_{0.38}N$. The red square (■) and black circle (●) represent the values of C concentrations of 1.8 × 10^{18} cm^{-3} and 6.5 × 10^{17} cm^{-3}, as grown under pressures 50 mbar and 100 mbar, respectively.

The difference in the forward voltages between TJ#3 and TJ#4 suggests that the Si overdose above 6 × 10^{19} cm^{-3} is effective for improving TJ despite the reduction in the carrier concentration with an increase of Si concentration, as shown in Figure 3b. The reduction of the carrier concentration can be attributed to the self-compensation of V_{III}–nSi complexes [17–22]. However, the depletion layer width was found to be reduced to approximately 10 nm for the Si doping concentration of 1.2 × 10^{20} cm^{-3} [38]. Therefore, the Si overdose can contribute to a reduction in the depletion layer width, which results in an increase in the tunneling probability. Another possibility is trap-assisted tunneling through defects formed by the Si overdose although a further investigation is required. Therefore, we concluded that both the C reduction and high Si doping are keys to reduce the forward voltage of AlGaN-based TJs.

The present TJ structure has very thick TJ layer compared to the depletion layer width of approximately 10 nm shown in Figure 1b, and it can be a cause of the excess series resistance of the n^+-type AlGaN layer. We further reduce the operation voltage to 8.8 V at a DC current of 63 A/cm^2 by optimizing the TJ thickness [39].

Preprints (www.preprints.org) | NOT PEER-REVIEWED | Posted: 15 February 2023 doi:10.20944/preprints202302.0249.v1

3.2. Sputtered Polycrystalline MgZnO/Al Reflective Electrodes for Enhanced Light Emission in AlGaN-based Homoepitaxial Tunnel Junction DUV-LED

We evaluate MgZnO/Al reflective electrodes for an $Al_{0.6}Ga_{0.4}N$ TJ LED (TJ#5) to enhance the LEE. The TJ LED of TJ#5 is performed under the optimized growth condition similar to that of TJ#4. These forward voltages are slightly increased by approximately 0.6 V when the Al composition of the p-type AlGaN increased from 50% (TJ#4) to 60% (TJ#5).

The current density–forward voltage characteristics of the AlGaN TJ LEDs using conventional Ti/Al and MgZnO electrodes are illustrated in Figure 4a. The forward voltages of the AlGaN TJ LEDs using Ti/Al and MgZnO/Al electrodes were 10.8 V and 10.3 V at a DC operation of 63 A/cm², respectively. The forward voltage offset of approximately 1 V was observed for the AlGaN TJ LED using MgZnO/Al electrodes compared with that using the Ti/Al electrodes at a current density of 30–60 A/cm². In addition, the forward voltages of the TJ LEDs of both Ti/Al and MgZnO/Al electrodes are comparable at a current density above 30 A/cm². Therefore, we realized carrier injection into the TJ LED using MgZnO/Al electrodes. For more details, the contact resistivity and band alignment of the interface between the MgZnO electrode and n-type AlGaN contact layer are reported in ref. [40].

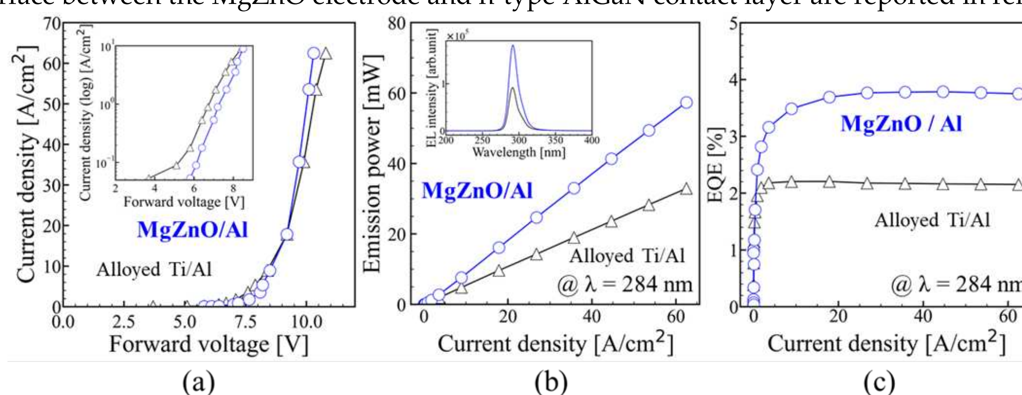

Figure 4. (**a**) Current density–forward voltage, (**b**) emission power–current density, and (**c**) EQE–current density characteristics of the fabricated TJ LEDs. Copyright 2022 The Japan Society of Applied Physics [40].

Figure 4b shows the current density–emission power characteristics and emission wavelength spectra of the AlGaN TJ LEDs. The emission wavelength is 284 nm at a DC operation of 63 A/cm². The output powers of the AlGaN TJ LEDs with conventional Ti/Al electrodes and MgZnO/Al electrodes are 32.8 and 57.3 mW, respectively, at a DC operation of 63 A/cm². The output power of the TJ LED using MgZnO/Al electrodes is enhanced to approximately 1.7 times using the Ti/Al electrodes. The external quantum efficiencies (EQEs) of the TJ LED using the Ti/Al electrodes and MgZnO/Al electrodes are 2.15% and 3.75%, respectively, at a DC operation of 63 A/cm², as shown in Figure 4c. The highest output power is realized for AlGaN TJ LEDs. A maximum EQE of 3.78% is achieved for the AlGaN TJ LED using MgZnO/Al electrodes. The reflectance at an emission wavelength of 284 nm for the TJ LED with the Ti/Al electrodes and MgZnO/Al electrodes was 9.5% and 20.2%, respectively. The Ti/Al electrodes exhibited low reflectivity because of the alloyed metal. In addition, the MgZnO/Al electrodes exhibited high reflectivity because of the nonalloyed Al separated from the cathode annealing process. Therefore, it contributed to the high reflectance of the TJ LED with MgZnO/Al electrodes.

Figure 5a shows the absorption coefficient spectrum of only the n-type $Al_{0.6}Ga_{0.4}N$ template and MgZnO (50 nm) on the n-type $Al_{0.6}Ga_{0.4}N$ template. The absorption coefficients of both increased near 4.8 eV. The absorption coefficient of MgZnO on the n-type $Al_{0.6}Ga_{0.4}N$ template increased near 4.0 eV. The band gap of wz-MgZnO is reported to be approximately 3.34–4.0 eV, which depends on the Mg composition [24]. The UV light absorption near 4.0 eV is attributed to wz-MgZnO. Figure 5(b) shows the thickness dependence of the transmittance of MgZnO based on the calculation from its absorption coefficient $\alpha = 1.6\times10^5$ cm^{-1} at the emission wavelength of 284 nm in the fabricated TJ LED. The transmittance of the MgZnO at a thickness of 50 nm is indicated as approximately 40%. We estimate

a transmittance of more than 80% by reducing the MgZnO thickness to less than 10 nm for enhancing the output power of AlGaN LEDs. The TJ LED structure can be optimized by utilizing optical cavity effects toward the improvement of LEE with other enhancement approaches [41,42]. The thickness of the n-type AlGaN in contact with the AlGaN TJ should be optimized in the near-future to realize a higher output power.

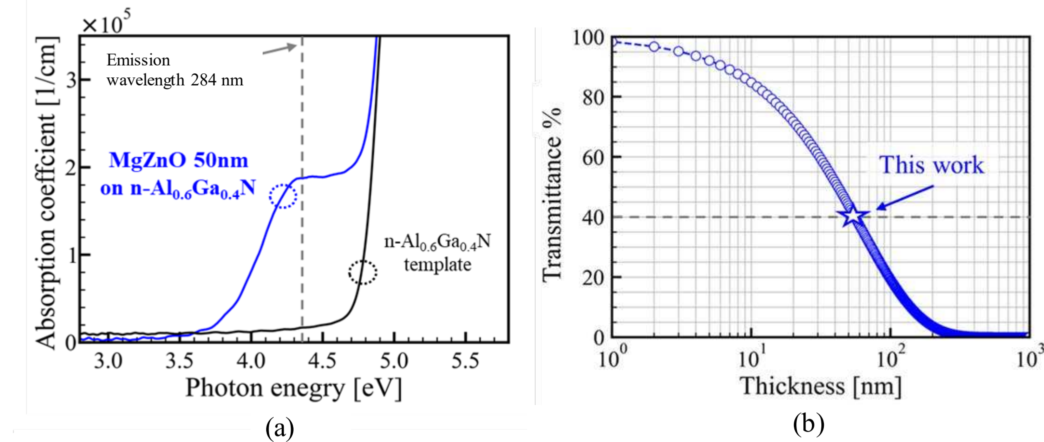

Figure 5. Comparison of the absorption coefficient spectra of the n-type $Al_{0.6}Ga_{0.4}N$ template and MgZnO deposited on the n-type $Al_{0.6}Ga_{0.4}N$. (**b**) Thickness dependence of the transmittance of MgZnO calculated from the absorption coefficient ($\alpha = 1.6 \times 10^5$ cm^{-1}) at a photon energy of 4.3 eV. Copyright 2022 The Japan Society of Applied Physics [40].

4. Conclusions

We realized the improvement of the high-Al-composition AlGaN TJ deep-UV LEDs by controlling the growth of n-type AlGaN and polycrystalline MgZnO/Al electrodes. Two essential factors are considered to reduce the operating voltage of AlGaN TJ LEDs by changing the growth condition: suppression of C incorporation and doping of n^+-type AlGaN at a high Si concentration. The operating voltage of AlGaN TJ LED was 10.8 V at a DC operation of 63 A/cm^2. Highly reflective MgZnO/Al electrodes were fabricated as anodes for AlGaN TJ LEDs to enhance the output power of the AlGaN TJ LEDs. The output power of the 57.3 mW of TJ LED using MgZnO/Al electrodes was realized at an emission wavelength of 284 nm under the DC operation of 63 A/cm^2; this was 1.7 times higher than that when using a conventional Ti/Al electrode. In the near future, the output power can be further improved by lessening the thickness of the MgZnO for AlGaN TJ LEDs.

Author Contributions: K. Nagata and T. Matsubara: writing–original draft preparation, K. Nagata, Y. Saito, M. Kushimoto, S. Tomai, S. Katsumata, Y. Honda, T. Takeuchi, and H. Amano; writing-review and editing, supervision, H. Amano. All authors have read and agreed to the published version of the manuscript.

Informed Consent Statement: Not applicable.

Acknowledgments: This work was supported by the MOE Program for the implementation of the innovative infection control and digital technologies with low CO_2 emission.

Conflicts of Interest: The authors declare no conflict of interest.

References

1. Oguma, K.; Rattanakul, S. UV inactivation of viruses in water: its potential to mitigate current and future threats of viral infectious diseases. *Jpn. J. Appl. Phys.* **2021**, *60*, 110502.
2. Minamikawa, T.; Koma, T.; Suzuki, A.; Nagamatsu, K.; Yasui, T.; Yasutomo, K.; Nomaguchi, M. Inactivation of SARS-CoV-2 by deep ultraviolet light emitting diode: A review. *Jpn. J. Appl. Phys.* **2021**, *60*, 090501.
3. Muramoto, Y.; Kimura, M.; Kondo, A. Verification of inactivation effect of deep-ultraviolet LEDs on bacteria and viruses, and consideration of effective irradiation methods. *Jpn. J. Appl. Phys.* **2021,** *60*, 090601.
4. Inagaki, H.; Saito, A.; Sugiyama, H.; Okabayashi, T.; Fujimoto, S. Rapid inactivation of SARS-CoV-2 with deep-UV LED irradiation. *Emerging Microbes Infect.* **2020,** *9*, 1744.

5. Saito, Y.; Wada, S.; Nagata, K.; Makino, H.; Boyama, S.; Miwa, H.; Matsui, S.; Kataoka, K.; Narita, T.; Horibuchi, K. Efficiency improvement of AlGaN-based deep-ultraviolet light-emitting diodes and their virus inactivation application. *Jpn. J. Appl. Phys.* **2021**, *60*, 080501.
6. Amano, H.; Collazo, R.; Santi, C. D.; Einfeldt, S.; Funato, M.; Glaab, J.; Hagedorn, S.; Hirano, A.; Hirayama, H.; Ishii, R.; Kashima, Y.; Kawakami, Y.; Kirste, R.; Kneissl, M.; Martin, R.; Mehnke, F.; Meneghini, M.; Ougazzaden, A.; J Parbrook, P.; Rajan, S.; Reddy, P.; Römer, F.; Rusche, J.; Sarkar, B.; Scholz, F.; J Schowalter, L. Shields, P.; Sitar, Z.; Sulmoni, L.; Wang, T.; Wernicke, T.; Weyers, M.; Witzigmann, B.; Wu, Y.; Wunderer, T.; and Zhang, Y.; The 2020 UV emitter roadmap. *J. Phys. D: Appl. Phys.* **2020**, *53*, 503001.
7. Ichikawa, M.; Endo, S.; Sagawa, H.; Fujioka, A.; Kosugi, T.; Mukai, T.; Uomoto, M.; Shimatsu, T. High-output-power deep ultraviolet light-emitting diode assembly using direct bonding. *ECS Trans.* **2016,** *75*, 53.
8. Muth, J. F.; Brown, J. D.; Johnson, M. A. L.; Yu, Z.; Kolbas, R. M.; Cook, Jr J. W.; Schetzina, J. F. Absorption coefficient and refractive index of GaN, AlN and AlGaN alloys. *MRS Internet J. Nitride Semicond. Res.* **1999**, *4S1*, G5.2.
9. Katsuragawa, M.; Sota, S.; Komori, M.; Anbe, C.; Takeuchi, T.; Sakai, H.; Amano, H.; Akasaki, I. Thermal ionization energy of Si and Mg in AlGaN. *J. Cryst. Growth* **1998**, *189/190*, 528.
10. Jeon, S. R.; Ren, Z.; Cui, G.; Su, J.; Gherasimova, M.; Han, J.; Cho, H. K.; Zhou, L. Investigation of Mg doping in high-Al content *p*-type $Al_xGa_{1-x}N$. *Appl. Phys. Lett.* **2005,** *86*, 082107.
11. Nakarmi, M. L.; Kim, K. H.; Khizar, M.; Fan, Z. Y.; Lin, J. Y.; Jiang, H. X. Electrical and optical properties of Mg-doped$Al_{0.7}Ga_{0.3}N$ alloys. *Appl. Phys. Lett.* **2005,** *86*, 092108.
12. Nakarmi, M. L.; Nepal, N.; Ugolini, C.; Altahtamouni, T. M.; Lin, J. Y.; Jiang, H. X. Correlation between optical and electrical properties of Mg-doped AlN epilayers. *Appl. Phys. Lett.* **2006**, *89*, 152120.
13. Szabó, Á; Son, N. T.; Janzén, E.; Gali, A. Stampfl, C.; Neugebauer, J.; Group-II acceptors in wurtzite AlN: A screened hybrid density functional study. *Appl. Phys. Lett.* **2010**, *96*, 192110.
14. Lyons, J. L.; Janotti, A.; Van de Walle, C. G. Shallow versus Deep Nature of Mg Acceptors in Nitride Semiconductors. *Phys. Rev. Lett.* **2012**, *108*, 156403.
15. Fan Arcara, V.; Damilano, B.; Feuillet, G.; Vézian, S.; Ayadi, K.; Chenot, S.; Duboz, J. Y. Ge doped GaN and $Al_{0.5}Ga_{0.5}N$-based tunnel junctions on top of visible and UV light emitting diodes. *J. Appl. Phys.* **2019**, *126*, 224503.
16. Kuhn, C.; Sulmoni, L.; Guttmann, M.; Glaab, J.; Susilo, N.; Wernicke, T.; Weyers, M.; Kneissl, M. MOVPE-grown AlGaN-based tunnel heterojunctions enabling fully transparent UVC LEDs. *Photon. Res*. **2019**, *7*, B7.
17. Nam, K. B.; Nakarmi, M. L.; Lin, J. Y.; Jiang, H. X. Photoluminescence studies of Si-doped AlN epilayers. *Appl. Phys. Lett.* **2005**, *86*, 222108.
18. Nepal, N.; Nakarmi, M. L.; Lin, J. Y.; Jiang, H. X. Photoluminescence studies of impurity transitions in AlGaN alloys. *Appl. Phys. Lett.* **2006,** *89*, 092107.
19. Chichibu, S. F.; Miyake, H.; Ishikawa, Y.; Tashiro, M.; Ohtomo, T.; Furusawa, K.; Hazu, K.; Hiramatsu, K.; Uedono, A. The origins and properties of intrinsic nonradiative recombination centers in wide bandgap GaN and AlGaN. *J. Appl. Phys.* **2013**, *113*, 213506.
20. Bryan, I.; Bryan, Z.; Washiyama, S.; Reddy, P.; Gaddy, B.; Sarkar, B.; Breckenridge, M. H.; Guo, Q.; Bobea, M.; Tweedie, J.; Mita, S.; Irving, D.; Collazo, R.; Sitar, Z. The role of transient surface morphology on composition control in AlGaN layers and wells. *Appl. Phys. Lett.* **2018,** *112*, 062102.
21. Nagata, K.; Makino, H.; Yamamoto, T.; Kataoka, K.; Narita, T.; Saito, Y. Low resistivity of highly Si-doped n-type $Al_{0.62}Ga_{0.38}N$ layer by suppressing self-compensation. *Appl. Phys. Exp.* **2020,** *13*, 025504.
22. Kataoka, K.; Narita, T.; Nagata, K.; Makino, H.; Saito, Y. Electronic degeneracy conduction in highly Si-doped $Al_{0.6}Ga_{0.4}N$ layers based on the carrier compensation effect. *Appl. Phys. Lett*. **2020**, *117*, 262103.
23. Sawada, N.; Narita, T.; Kanechika, M.; Uesugi, T.; Kachi, T.; Horita, M.; Kimoto, T.; Suda, J. Sources of carrier compensation in metalorganic vapor phase epitaxy-grown homoepitaxial n-type GaN layers with various doping concentrations. *Appl. Phys. Exp.* **2018**, *11*, 041001.
24. Wang, X.; Saito, K.; Tanaka, T.; Nishio, M.; Nagaoka, T.; Arita, M.; Guo, Q. Energy band bowing parameter in MgZnO alloys. *Appl. Phys. Lett.* **2015,** *107*, 022111.
25. Wang, X.; Saito, K.; Tanaka, T.; Nishio, M.; Guo, Q. Lower temperature growth of single phase MgZnO films in all Mg content range. *J. Alloys Compd.* **2015,** *627*, 383.
26. Kushimoto, M.; Sakai, T.; Ueoka, Y.; Tomai, S.; Katsumata, S.; Deki, M.; Honda, Y.; Amano, H. Effect of annealing on the electrical and optical properties of MgZnO films deposited by radio frequency magnetron sputtering. *Phys. Status Solidi A* **2020,** *217*, 1900955.
27. Imura, M.; Nakano, K.; Fujimoto, N.; Okada, N.; Balakrishnan, K.; Iwaya, M.; Kamiyama, S.; Amano, H.; Akasaki, I.; Noro, T.; Takagi, T.; Bandoh, A. Dislocations in AlN Epilayers Grown on Sapphire Substrate by High-Temperature Metal-Organic Vapor Phase Epitaxy. *Jpn. J. Appl. Phys.* **2007,** *46*, 1458.
28. Nagata, K.; Makino, H.; Yamamoto, T.; Saito, Y.; Miki, H. Origin of optical absorption in AlN with air voids. *Jpn. J. Appl. Phys.* **2019,** *58*, SCCC29.

Preprints (www.preprints.org) | NOT PEER-REVIEWED | Posted: 15 February 2023 doi:10.20944/preprints202302.0249.v1

29. Kuwano, Y.; Kaga, M.; Morita, T.; Yamashita, K.; Yagi, K.; Iwaya, M.; Takeuchi, T.; Kamiyama, S.; Akasaki, I. Lateral hydrogen diffusion at p-GaN layers in nitride-based light emitting diodes with tunnel junctions. *Jpn. J. Appl. Phys.* **2013**, *52*, 08JK12.
30. Neugebauer, S.; Hoffmann, M. P.; Witte, H.; Bläsing, J.; Dadgar, A.; Strittmatter, A.; Niermann, T.; Narodovitch, M.; Lehmann, M. All metalorganic chemical vapor phase epitaxy of p/n-GaN tunnel junction for blue light emitting diode applications. *Appl. Phys. Lett.* **2017**, *110*, 102104.
31. Hwang, D.; Mughal, A. J.; Wong, M. S.; Alhassan, A. I.; Nakamura, S.; DenBaars, S. P. Micro-light-emitting diodes with III–nitride tunnel junction contacts grown by metalorganic chemical vapor deposition. *Appl. Phys. Exp.* **2018**, *11*, 012102.
32. Alhassan, A. I.; Young, E. C.; Alyamani, A. Y.; Albadri, A.; Nakamura, S.; DenBaars, S. P.; Speck, J. S. Reduced-droop green III–nitride light-emitting diodes utilizing GaN tunnel junction. *Appl. Phys. Exp.* **2018**, *11*, 042101.
33. Narita, T.; Tomita, K.; Yamada, S.; Kachi, T. Quantitative investigation of the lateral diffusion of hydrogen in p-type GaN layers having NPN structures. *Appl. Phys. Exp.* **2019**, *12*, 011006.
34. Nagata, K.; Makino, H.; Miwa, H.; Matsui, S.; Boyama, S.; Saito, Y.; Kushimoto, M.; Honda, Y.; Takeuchi, T.; Amano, H. Reduction in operating voltage of AlGaN homojunction tunnel junction deep-UV light-emitting diodes by controlling impurity concentrations. *Appl. Phys. Exp.* **2021**, *14*, 084001.
35. Inazu, T.; Fukahori, S.; Pernot, C.; Kim, M. H.; Fujita, T.; Nagasawa, Y.; Hirano, A.; Ippommatsu, M.; Iwaya, M.; Takeuchi, T.; Kamiyama, S.; Yamaguchi, M. Honda, Y.; Amano, H.; Akasaki, I. Improvement of light extraction efficiency for AlGaN-based deep ultraviolet light-emitting diodes. *Jpn. J. Appl. Phys.* **2011**, *50*, 122101.
36. Sung, Y. J.; Kim, M.; Kim, H.; Choi, S.; Kim, Y. H.; Jung, M.; Choi, R.; Moon, Y.; Oh, J.; Jeong, H.; Yeom, G. Y. Light extraction enhancement of AlGaN-based vertical type deep-ultraviolet light-emitting-diodes by using highly reflective ITO/Al electrode and surface roughening. *Opt. Exp.* **2019**, *27*, 29930.
37. Lee, S. Y.; Han, D. S.; Lee, Y. G.; Choi, K. K.; Oh, J. T.; Jeong, H. H.; Seong, T. Y.; Amano, H. Heavy Mg Doping to Form Reliable Rh Reflective Ohmic Contact for 278 nm Deep Ultraviolet AlGaN-Based Light-Emitting Diodes. *ECS J. Solid State Sci. Technol.* **2020**, *9*, 065016.
38. Nagata, K.; Anada, S.; Saito, Y.; Kushimoto, M.; Honda, Y.; Takeuchi, T.; Yamamoto, K.; Hirayama, T.; Amano, H. Visualization of depletion layer in AlGaN homojunction p–n junction. *Appl. Phys. Exp.* **2022**, *15*, 036504.
39. Nagata, K.; Anada, S.; Miwa, H.; Matsui, S.; Boyama, S.; Saito, Y.; Kushimoto, M.; Honda, Y.; Takeuchi, T.; Amano, H. Structural design optimization of 279 nm wavelength AlGaN homojunction tunnel junction deep-UV light-emitting diode. *Appl. Phys. Exp.* **2022**, *15*, 044003.
40. Matsubara, T.; Nagata, K.; Kushimoto, M.; Tomai, S.; Katsumata, S.; Honda, Y.; Amano, H. Sputtered polycrystalline MgZnO/Al reflective electrodes for enhanced light emission in AlGaN-based homojunction tunnel junction DUV-LED. *Appl. Phys. Exp.* **2022**, *15*, 044001.
41. Shen Y. C.; Wierer, J. J.; Krames, M. R.; Ludowise, M. J.; Misra, M. S.; Ahmed, F. Kim, A. Y.; Mueller, G. O.; Bhat, J. C.; Stockman, S. A.; Martin, P. S. Optical cavity effects in InGaN/GaN quantum-well-heterostructure flip-chip light-emitting diodes. *Appl. Phys. Lett.* **2003**, *82*, 2221.
42. Matsukura, Y.; Inazu, T.; Pernot, C.; Shibata, N.; Kushimoto, M.; Deki, M.; Honda, Y.; Amano, H. Improving light output power of AlGaN-based deep-ultraviolet light-emitting diodes by optimizing the optical thickness of p-layers. *Appl. Phys. Exp.* **2021**, *14*, 084004.

Disclaimer/Publisher's Note: The statements, opinions and data contained in all publications are solely those of the individual author(s) and contributor(s) and not of MDPI and/or the editor(s). MDPI and/or the editor(s) disclaim responsibility for any injury to people or property resulting from any ideas, methods, instructions or products referred to in the content.